

Spherical spin-orientation degeneracy of basic antiferromagnetic configurations due to the dipolar interaction in cubic lattices

Eugene V. Kholopov*

Institute of Inorganic Chemistry of the Siberian Branch of the Russian Academy of Sciences, 630090 Novosibirsk, Russia

Based on a simple general relation for the Lorentz field, the precise values are obtained for the energies of ferromagnetic and basic antiferromagnetic states in sc, bcc, fcc, and diamond cubic lattices. Within both the 'nearest-neighbor' and group-theoretic approaches, a large variety of antiferromagnetic states revealed as corresponding to the lowest energies is addressed, with recognizing their spherical spin-orientation degeneracy, which turns out to be rather special in fcc lattices.

PACS numbers: 75.10.Hk, 75.25.+z, 81.40.Rs

The dipolar interaction of spins is typical of dilute magnets [1] and so remains actual upon describing modern complex compounds where the direct exchange is either depressed [2, 3, 4, 5] or frustrated [6]. In this connection, dipolar solutions in cubic structures are interesting themselves [3, 4, 7, 8] and also enable one to understand magnetic ordering in structures of a lower symmetry [5, 9, 10, 11]. It is known that antiferromagnetic ground states are typical of the sc [12] and diamond [13] structures, whereas the bcc and fcc lattices are ferromagnetic [4, 12, 14] in the thermodynamic limit [5, 13, 15, 16].

In order to describe basic spin configurations, the 'nearest-neighbor' [12] and group-theoretic [14] treatments are usually applied [5]. However, an explicit motif of spin arrangement in shortest-distance directions [12], that is characteristic of the dipolar interaction, is not still recognized in the bcc lattice. Nevertheless, the same motif gives rise to the widespread standpoint that basic antiferromagnetic arrangements are attached to crystallographic axes [5, 13, 17]. This is at odds with spherical degeneracy of ferromagnetic configurations [4], as well as with the fact that the spherical degeneracy of antiferromagnetic states in sc lattices has already been proved [14]. This is the reason that here we study this question addressed to all cubic lattices in a systematic manner, with treating spins as classical vectors.

As for the problem of summation of dipolar lattice series that is rather tedious conventionally [5, 18, 19], here we propose a simple general approach based on introducing fictitious charges [20]. Let us consider the general case of a triclinic crystal with lattice constants a , b , and c along non-orthogonal triclinic directions \mathbf{e}_a , \mathbf{e}_b , and \mathbf{e}_c , respectively, and with n moments \mathbf{M}_j localized at the positions \mathbf{t}_j in a unit cell, providing that \mathbf{M}_j can differ from one other. Concentrating on a j th sublattice built up of parallel moments \mathbf{M}_j at a given j , it is expedient to cast \mathbf{M}_j in terms of triclinic coordinates

$$\mathbf{M}_j = M_{ja}\mathbf{e}_a + M_{jb}\mathbf{e}_b + M_{jc}\mathbf{e}_c \equiv [M_{ja}, M_{jb}, M_{jc}], \quad (1)$$

where the square brackets are used in order to distinguish this representation from a Cartesian one. Then the unit cell of this sublattice, with \mathbf{M}_j at its center, can be mod-

ified by three point charge species

$$q_{j1} = -\frac{M_{ja}}{a}, \quad q_{j2} = -\frac{M_{jb}}{b}, \quad q_{j3} = -\frac{M_{jc}}{c} \quad (2)$$

at the unit-cell positions

$$\mathbf{r}_1 = [\frac{1}{2}a, 0, 0], \quad \mathbf{r}_2 = [0, \frac{1}{2}b, 0], \quad \mathbf{r}_3 = [0, 0, \frac{1}{2}c], \quad (3)$$

but the charges $-q_{j1}$, $-q_{j2}$, and $-q_{j3}$ are assumed at $-\mathbf{r}_1$, $-\mathbf{r}_2$, and $-\mathbf{r}_3$, respectively. As a result, one can see that the total dipolar moment of the unit cell is zero and all the charges above cancel one other upon summing over the lattice. Therefore, the field exerted by this modified sublattice on any moment \mathbf{M} at the position \mathbf{t} is determined by the convergent lattice series, which can be easily obtained from the appropriate expansion of a Coulomb lattice series, as will be discussed elsewhere [21]. This is a generalized Lorentz field of the form

$$\mathbf{L}_j(\mathbf{t}) = \sum_i' \left\{ \left[\frac{3((\mathbf{R}_i - \mathbf{t})\mathbf{M}_j)(\mathbf{R}_i - \mathbf{t})}{|\mathbf{R}_i - \mathbf{t}|^5} - \frac{\mathbf{M}_j}{|\mathbf{R}_i - \mathbf{t}|^3} \right] + \sum_m q_{jm} \left[\frac{\mathbf{R}_i - \mathbf{r}_m - \mathbf{t}}{|\mathbf{R}_i - \mathbf{r}_m - \mathbf{t}|^3} - \frac{\mathbf{R}_i + \mathbf{r}_m - \mathbf{t}}{|\mathbf{R}_i + \mathbf{r}_m - \mathbf{t}|^3} \right] \right\}, \quad (4)$$

where the summation is over the j th sublattice described by \mathbf{R}_i , the prime on the summation sign implies missing the cases of zero denominators, $((\mathbf{R}_i - \mathbf{t})\mathbf{M}_j)$ stands for the scalar product. The first term in the curly braces in (4) is the direct sum of dipole contributions and the second one is the Lorentz field itself that is responsible for the topological boundary effects [16]. Note that the convergence of (4) takes place if the summation over i is the outer procedure. Keeping (4) in mind and taking all the sublattices into account, the total bulk dipolar energy per unit cell is as follows:

$$\mathcal{E} = -\frac{1}{2} \sum_{j_1, j_2} (\mathbf{M}_{j_1} \mathbf{L}_{j_2}(\mathbf{t}_{j_1} - \mathbf{t}_{j_2})). \quad (5)$$

Here we focus on the four cubic structures with the lattice spacing a : the sc, bcc, fcc, and diamond ones. The volume v_s per spin is equal to a^3 , $a^3/2$, $a^3/4$, and $a^3/8$, respectively. All the spin values $|\mathbf{M}|$ are supposed to be

TABLE I: The bulk dipolar energy \mathcal{E}_s per spin in units of \mathbf{M}^2/v_s for the ferro- (F) and basic antiferromagnetic (AF) states in cubic structures, with indicating the three- (3D) and two-dimensional (2D) degeneracy in the latter case.

Structure	\mathcal{E}_s (F) ^a	\mathcal{E}_s (AF)	AF degeneracy	
			3D ^a	2D ^b
sc	-2.094395 ^c	-2.676789	1 ^d	—
bcc	-2.094395 ^c	-1.985921 ^e	2	3 ^d
fcc	-2.094395 ^c	-1.807574	4 ^f	3 ^{d,g} + 3 ^h
diamond	-2.094395 ^c	-3.196851	2	3 ^d

^aThe direction of a reference spin species is arbitrary.

^bReference spins lie in one of the three basal planes.

^cThis is just the value of $-2\pi/3$, in accord with (6) [14].

^dHere the cases are contained of collinear spins inherent in the sc [12], bcc [21], fcc [12], and diamond [13] lattices.

^eThis value was discussed earlier [14] as associated with spins along different crystallographic axes in the two sc sublattices.

^fTwo-parameter sets of states at a given reference spin.

^gOne-parameter continuous sets of states.

^hOne-parameter piecewise continuous sets of states.

the same, so that the energy per spin $\mathcal{E}_s = \mathcal{E}/n$ is of interest. The energies for ferromagnetic spin arrangements calculated from (2)–(5) are shown in Table I and agree with the fact that the direct dipole contribution to (4) upon summation over cubic shells is zero by symmetry, so that the bulk dipolar energy per spin is reduced to the contribution of the Lorentz field itself [22]:

$$\mathcal{E}_s = -\frac{2\pi\mathbf{M}^2}{3v_s}. \quad (6)$$

This approach is also fruitful upon calculating basic antiferromagnetic states, which can be decomposed into sc ferromagnetic sublattices. The results are exhibited in Table I as well. To address a large variety of such states revealed, we resort to the description of Luttinger and Tisza [14], in terms of which the sc antiferromagnetic structure is described by the state

$$(\alpha X_5 + \beta Y_5 + \gamma Z_5), \quad \alpha^2 + \beta^2 + \gamma^2 = 1 \quad (7)$$

with the energy per spin proportional to [14]

$$\alpha^2 + \beta^2 + \gamma^2. \quad (8)$$

According to the definition of X_5 , Y_5 , and Z_5 , it implies the three-dimensional (3D) degeneracy of this antiferromagnetic (AF) state shown in Fig. 1 (a), with local moments, in units of $|\mathbf{M}|$, of the form [14]

$$\begin{aligned} \mathbf{a} &= (\alpha, \beta, \gamma), & \mathbf{b} &= (\alpha, -\beta, -\gamma), \\ \mathbf{c} &= (-\alpha, \beta, -\gamma), & \mathbf{d} &= (-\alpha, -\beta, \gamma). \end{aligned} \quad (9)$$

The basic AF bcc structure is unstable, in agreement with Table I. Nevertheless, it can be specified in the same manner. If the two sc sublattices are described by the states

$$(\alpha X_7 + \beta Y_7 + \gamma Z_7), \quad (\xi X_6 + \eta Y_6 + \zeta Z_6) \quad (10)$$

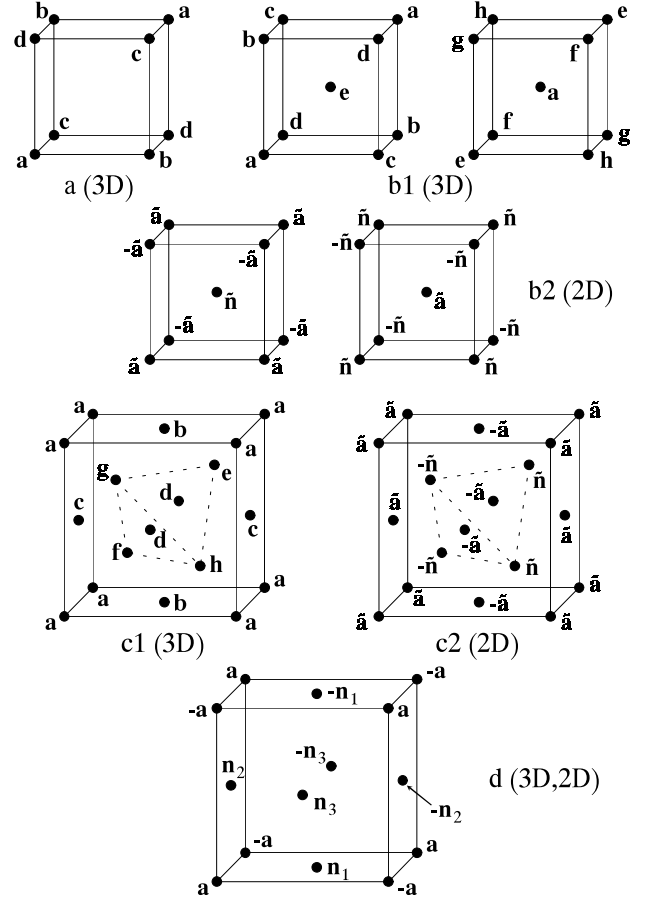


FIG. 1: 3D basic antiferromagnetic configurations in the sc (a), bcc (b1), and diamond (c1) structures, with spins specified by (9) and (12). 2D configurations typical of the bcc (b2) and diamond (c2) structures contain spins driven by (14). A basic antiferromagnetic fcc structure (d) is common to 3D and 2D configurations described by (15) and either by (20)–(23) or by (28)–(30) as an example, respectively.

normalized like (7), then the energy of interaction of these sublattices is specified by [14]

$$\max\{\alpha\eta + \beta\zeta + \gamma\xi\} \rightarrow \xi = \gamma, \quad \eta = \alpha, \quad \zeta = \beta, \quad (11)$$

for the expression in the curly braces can be treated as a scalar product of two unit vectors which must be parallel. It implies the 3D configuration shown in Fig. 1 (b1), where apart from (9), the local spin states defined as

$$\begin{aligned} \mathbf{e} &= (\gamma, \alpha, \beta), & \mathbf{f} &= (\gamma, -\alpha, -\beta), \\ \mathbf{g} &= (-\gamma, \alpha, -\beta), & \mathbf{h} &= (-\gamma, -\alpha, \beta) \end{aligned} \quad (12)$$

take place. The interchange of the two sublattices leads to the twofold degeneracy of such states, as shown in Table I. In other words, the two rotations of the lattice in Fig. 1 (a) about the (1,1,1) axis, but without rotating spins, generate the first sublattice here. It is worth noting that the particular cases of \mathbf{a} along one of the four cubic diagonals are associated with the idea of Sauer [12]

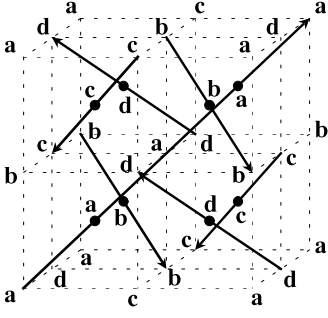


FIG. 2: The structure of interpenetrating ferromagnetic chains shown by the solid arrows in the nearest-neighbor directions as a particular case of Fig. 1 (b1) at $\mathbf{a} = (\frac{1}{\sqrt{3}}, \frac{1}{\sqrt{3}}, \frac{1}{\sqrt{3}})$. The first sublattice is depicted by the dotted lines, whereas the filled circles exhibit the second sublattice.

about ferromagnetic chains along the nearest neighbors, as shown in Fig. 2, where the cubic chain packing appears to be similar to the chain cubic structure intrinsic in TiHF_2 at low temperatures [23].

Another possibility is associated with the states

$$(\beta Y_7 + \gamma Z_6), \quad (\gamma Y_7 + \beta Z_6), \quad (13)$$

which imply the configuration shown in Fig. 1 (b2) at

$$\tilde{\mathbf{a}} = (0, \beta, \gamma), \quad \tilde{\mathbf{n}} = (0, \gamma, \beta). \quad (14)$$

The cyclic interchange of the parameters in (14) explains the threefold degeneracy of this two-dimensional (2D) set, as indicated in Table I. Note that all the states above follow from the 'nearest-neighbor' treatment of Sauer [12] as well and this set of possibilities is complete.

The same 'nearest-neighbor' treatment enables us to extend the solution typical of the bcc structure to the diamond one. Indeed, any sc lattice can be regarded as a combination of two fcc sublattices, as it happens in the NaCl structure, but with equal energy effects at body-centered positions. So, upon removing one of the fcc sublattices from either of the sc sublattices in the bcc structure, a diamond structure arises. As a result, the total set of solutions for the diamond structure is still defined either by (9) and (12), or by (14), as shown in Fig. 1 (c1) and Fig. 1 (c2), respectively, with the corresponding degrees of degeneracy. The chain structure similar to that in Fig. 2, but with two alternating spin-spin distances along every chain, takes place here as well.

For completeness, we also consider the fcc lattice, where the situation turns out to be much more complicated and dramatic. In terms of unit vectors \mathbf{a} , \mathbf{n}_1 , \mathbf{n}_2 , and \mathbf{n}_3 specifying four sc sublattices of the same form, both the above treatments predict the limiting antiferromagnetic structure drawn in Fig. 1 (d). On introducing the unit vector components along the principal axes:

$$\mathbf{a} = (\alpha, \beta, \gamma), \quad \mathbf{n}_l = (\xi_l, \eta_l, \zeta_l), \quad (15)$$

one can show that the lowest energy of such a structure corresponds to the condition

$$(\eta_1 + \zeta_3 - \alpha)^2 + (\xi_1 + \zeta_2 - \beta)^2 + (\xi_3 + \eta_2 - \gamma)^2 + (\xi_2 + \eta_3 + \zeta_1)^2 = 0, \quad (16)$$

with the obvious solutions

$$\begin{aligned} \eta_1 + \zeta_3 - \alpha &= 0, & \xi_1 + \zeta_2 - \beta &= 0, \\ \xi_3 + \eta_2 - \gamma &= 0, & \xi_2 + \eta_3 + \zeta_1 &= 0. \end{aligned} \quad (17)$$

Further it is expedient to write down the unit vector normalization in the form

$$\xi_l = A_l, \quad \eta_l = C_l P_l, \quad \zeta_l = C_l Q_l, \quad (18)$$

$$A_l^2 + C_l^2 + 1, \quad P_l^2 + Q_l^2 = 1 \quad (19)$$

corresponding to spherical coordinates. According to (16) and (19), it is clear that apart from the reference unit vector \mathbf{a} , which is assumed to be arbitrary, two additional parameters describing (18) remain variable as well. In particular, we choose $\xi_1 \equiv A$ and $\xi_2 \equiv B$ as such parameters here. On substituting (18) into (17) and resolving those relations with account of (19), one can show that the other components take the form

$$\zeta_2 = \beta - A, \quad (20)$$

$$\begin{cases} \eta_2 = \pm \sqrt{1 - (\beta - A)^2 - B^2}, \\ \xi_3 = \gamma \mp \sqrt{1 - (\beta - A)^2 - B^2}, \end{cases} \quad (21)$$

$$\begin{cases} \eta_1 = \frac{-\alpha(A^2 - \xi_3^2 - \alpha^2 - B^2) \pm B\Omega}{2(\alpha^2 + B^2)}, \\ \zeta_1 = \frac{B(A^2 - \xi_3^2 - \alpha^2 - B^2) \pm \alpha\Omega}{2(\alpha^2 + B^2)}, \\ \eta_3 = \frac{-B(A^2 - \xi_3^2 + \alpha^2 + B^2) \mp \alpha\Omega}{2(\alpha^2 + B^2)}, \\ \zeta_3 = \frac{\alpha(A^2 - \xi_3^2 + \alpha^2 + B^2) \mp B\Omega}{2(\alpha^2 + B^2)}, \end{cases} \quad (22)$$

$$\Omega = \sqrt{4(1 - A^2)(\alpha^2 + B^2) - (A^2 - \xi_3^2 - \alpha^2 - B^2)^2}, \quad (23)$$

where the choice of an upper or lower sign is common to both the relations (21) and the same is right for all four relations (22), which case is independent of (21). Altogether, four two-parameter sets of solutions as functions of α , β , and γ exist, as pointed out in Table I. The change in A and B is restricted by the following inequalities:

$$|A| \leq 1, \quad \mp 2\gamma - \gamma^2 \leq (\beta - A)^2 + B^2 \leq 1, \quad (24)$$

$$(A^2 - \xi_3^2 - \alpha^2 - B^2)^2 \leq 4(1 - A^2)(\alpha^2 + B^2) \quad (25)$$

which emerge from (19) and from the conditions that the square roots in (21) and (23) be real, an upper or lower sign in (24) agrees with that in (21).

In particular, if $A = \beta$ and $B = \lambda = \pm 1$, then relations (24) and (25) hold automatically and solutions (20)–(23)

are reduced to

$$\eta_2 = \zeta_2 = 0, \quad \xi_3 = \gamma, \quad (26)$$

$$\begin{cases} \eta_1 = \frac{\alpha(1 - \beta^2) \pm \lambda\sqrt{(1 - \beta^2)(1 - \gamma^2)}}{1 + \alpha^2}, \\ \zeta_1 = \frac{\lambda(\beta^2 - 1) \pm \alpha\sqrt{(1 - \beta^2)(1 - \gamma^2)}}{1 + \alpha^2}, \\ \eta_3 = \frac{\lambda(\gamma^2 - 1) \mp \alpha\sqrt{(1 - \beta^2)(1 - \gamma^2)}}{1 + \alpha^2}, \\ \zeta_3 = \frac{\alpha(1 - \gamma^2) \mp \lambda\sqrt{(1 - \beta^2)(1 - \gamma^2)}}{1 + \alpha^2}. \end{cases} \quad (27)$$

The existence of four branches of solutions (20)–(23) ensues from (26)–(27) by continuity.

The case of $\alpha = B = 0$ implies $\tilde{\mathbf{a}} = (0, \beta, \gamma)$ and $\tilde{\mathbf{n}}_2 = (0, \eta_2, \zeta_2)$. It is degenerate in the representation at hand and can be studied directly from (17) giving rise to

$$\eta_3 = -\zeta_1, \quad \zeta_3 = -\eta_1, \quad \eta_1^2 + \zeta_1^2 = 1 - \xi_1^2. \quad (28)$$

According to (19), there are two solutions for the other components here. The first one is defined by

$$\xi_1 = \xi_3 = 0, \quad \eta_2 = \gamma, \quad \zeta_2 = \beta, \quad (29)$$

in which case the consistent rotation of $\tilde{\mathbf{a}}$ and $\tilde{\mathbf{n}}_2$ in the plane normal to the first axis is accompanied by an independent consistent rotation of the couple of \mathbf{n}_1 and \mathbf{n}_3 in the same plane. In other words, (28) and (29) generate a one-parameter continuous solution. The second solution in question is of the form

$$\begin{cases} \xi_1 = -\xi_3 = \beta - \gamma, & \tilde{\mathbf{n}}_2 = \tilde{\mathbf{a}} & \text{at } \beta\gamma > 0, \\ \xi_1 = \xi_3 = \beta + \gamma, & \tilde{\mathbf{n}}_2 = -\tilde{\mathbf{a}} & \text{at } \beta\gamma < 0. \end{cases} \quad (30)$$

According to (28) and (30), one can see that an independent consistent precession of \mathbf{n}_1 and \mathbf{n}_3 about the first axis is admissible, while both β and γ are nonzero and so determine the angle of precession. In this case the rotations of both $\tilde{\mathbf{a}}$ and $\tilde{\mathbf{n}}_2$ are connected. But if either β or γ goes through zero, then $\tilde{\mathbf{n}}_2$ undergoes the sudden inversion. At those moments the precession of \mathbf{n}_1 and \mathbf{n}_3 disappears: both \mathbf{n}_1 and \mathbf{n}_3 are along the first axis and one of them is inverted in a jump-like manner as well.

Note that the solutions of similar types are to be expected at $\beta = \eta_3 = 0$ and $\gamma = \zeta_1 = 0$. This is the reason that all three pairs of these one-parameter two-dimensional solutions are pointed out in Table I, though the latter solutions, with including piecewise continuous ones, are contained in the general case of (20)–(23).

In summary, both the ‘nearest-neighbor’ and group-theoretic approaches are suitable for investigating the lowest energy antiferromagnetic configurations. The latter one appears to be more effective upon describing the

sc and bcc lattices, but the former is favorable for extending the foregoing results to the diamond case. Of course, the spherical degeneracy discussed is the most important for antiferromagnetic ground states in the sc and diamond lattices, where it accounts for the high isotropic susceptibility recorded experimentally [13]. On the other hand, the spherical degeneracy revealed is a general property of the cubic symmetry. Thus the peculiar features of the foregoing results relevant to the sc, bcc, and fcc lattices are to be important for understanding the energy splitting upon lowering the lattice symmetry.

* Electronic address: kholopov@casper.che.nsk.su

- [1] J. H. Van Vleck, J. Chem. Phys. **5**, 320 (1937).
- [2] Th. Niemeijer, Physica **57**, 281 (1972).
- [3] L. M. Holmes, J. Als-Nielsen, and H. J. Guggenheim, Phys. Rev. B **12**, 180 (1975).
- [4] M. R. Roser and L. R. Corruccini, Phys. Rev. Lett. **65**, 1064 (1990).
- [5] J. F. Fernández and J. J. Alonso, Phys. Rev. B **62**, 53 (2000).
- [6] S. E. Palmer and J. T. Chalker, Phys. Rev. B **62**, 488 (2000).
- [7] Th. Niemeijer and H. W. J. Blöte, Physica **67**, 125 (1973).
- [8] V. Massidda, Physica B **145**, 124 (1987).
- [9] M. H. Cohen and F. Keffer, Phys. Rev. **99**, 1135 (1955).
- [10] N. M. Fujiki, K. De’Bell, and D. J. W. Geldart, Phys. Rev. B **36**, 8512 (1987).
- [11] D. Steiger, C. Ahlbrandt, and R. Glaser, J. Phys. Chem. B **102**, 4257 (1998).
- [12] J. A. Sauer, Phys. Rev. **57**, 142 (1940).
- [13] S. J. White, M. R. Roser, J. Xu, J. T. van der Noordaa, and L. R. Corruccini, Phys. Rev. Lett. **71**, 3553 (1993).
- [14] J. M. Luttinger and L. Tisza, Phys. Rev. **70**, 954 (1946); **72**, 257(E) (1947).
- [15] R. B. Griffiths, Phys. Rev. **176**, 655 (1968).
- [16] E. V. Kholopov, Physics–Uspekhi (2004), to be published.
- [17] J. P. Bouchaud and P. G. Zerah, Phys. Rev. B **47**, 9095 (1993).
- [18] P. Brüesch and M. Lietz, J. Phys. Chem. Solids **31**, 1137 (1970).
- [19] J. H. P. Colpa, Physica **56**, 185; 205 (1971).
- [20] H. M. Evjen, Phys. Rev. **39**, 675 (1932).
- [21] E. V. Kholopov, Preprint 2001-02 (Inst. of Inorg. Chem., Novosibirsk, 2001).
- [22] H. A. Lorentz, *The Theory of Electrons* (Teubner, Leipzig, 1916).
- [23] E. V. Kholopov, A. M. Panich, N. K. Moroz, and Yu. G. Kriger, Zh. Eksp. Teor. Fiz. **84**, 1091 (1983) [Sov. Phys.–JETP **57**, 632 (1983)].